For acidified Me_2SO solution the lifetime data in Table II yield an activation energy of 12 kcal mol^{-1} over the range 29.4–50.2 °C; while those for 0.10 M $HClO_4$ provide a value of 14 kcal mol^{-1} between 19.9 and 50.0 °C. The corresponding values reported for *trans*-Cr(cyclam)$(NH_3)_2^{3+}$ in Me_2SO (H^+) and 0.10 M $HClO_4$ are 16 and 18 kcal mol^{-1}, respectively.

These data are accommodated by a doublet excited-state relaxation model proposed by Endicott and co-workers[21-23] involving thermally activated surface crossing to a ground-state intermediate species, with subsequent partitioning between a reaction decay channel and nonradiative relaxation, which regenerates the parent ground state. For systems with highly constrained ligands, the reaction channel may be largely eliminated, which may result in very low reaction quantum yields. This possibility rationalizes the photobehavior of *trans*-Cr(cyclam)$(NH_3)_2^{3+}$,[1] Cr(sep)$_3^{3+}$,[21-23] and Cr((9)aneN$_3$)$_2^{3+}$ [24] (where sep is a sepulchrate ligand and (9)aneN$_3$ is 1,4,7-triazacyclononane). For *trans*-Cr(tet a)$(NH_3)_2^{3+}$ a lower activation energy for doublet ⟿ intermediate surface crossing than that for the cyclam analogue is in accord with the lifetime temperature dependencies and could result in a more prominent role for this decay process at room temperature. Such a situation would account for the shorter emission lifetimes of *trans*-Cr(tet a)$(NH_3)_2^{3+}$ in room-temperature solution, while the cyclam and tet a complexes have essentially identical lifetimes at 77 K (Table II).

***trans*-[Rh(tet a)$(CN)_2$]ClO_4·H_2O.** Under D_{4h} symmetry the lowest lying excited state, $^3T_{1g}$ (O_h), is split into ^3E_g and $^3A_{2g}$ sublevels. Since the $^3A_{2g}$ component is expected to be lower lying,[5] photolabilization should be primarily associated with Rh–amine bond cleavage. As found for its cyclam analogue,[5] the compound is essentially photoinert under LF excitation—an observation that attests to the effectiveness of such macrocyclic rings in eliminating amine ligand release. The compound displays a strong, broad, structureless emission centered at 480 nm in room-temperature aqueous, or Me_2SO solution, similar to that of *trans*-Rh(cyclam)$(CN)_2^+$, which is assigned to $^3A_{2g} \rightarrow {}^1A_{1g}$ (D_{4h}) phosphorescence. The emission is quenched in strongly basic solution and regenerated on reacidification.

At 20 °C and 280-nm excitation, the steady-state emission intensity of an acidified aqueous solution of *trans*-Rh(tet a)$(CN)_2^+$ was 0.46 times that of an absorbance matched solution of *trans*-Rh(cyclam)$(CN)_2^+$. The emission lifetimes are exceptionally long by normal Rh(III) standards.[5] The lifetime in acidified aqueous solution at 20 °C is 0.57 times that of *trans*-Rh(cyclam)$(CN)_2^+$, while their lifetimes are comparable at 77 K (Table II). These room-temperature differences are accompanied by substantial differences in the apparent activation energies for emission. Aqueous lifetime data from 12.3 to 53.0 °C yield an activation energy of 9.0 kcal mol^{-1} for the cyclam species, while the tet a value from 11.2 to 39.0 °C is only 6.0 kcal mol^{-1}. A thermally activated process such as $^3A_{2g}$ ⟿ ^3E_g internal back-conversion may be an important $^3A_{2g}$ relaxation pathway near room temperature—the smaller tet a energy gap then accounting for the compound's shorter lifetime and smaller steady-state emission intensity at 20 °C.

It is tempting to link the enhanced room-temperature emission intensity and lifetime of *trans*-Rh(cyclam)$(CN)_2^+$ and *trans*-Rh(tet a)$(CN)_2^+$ with elimination of the $^3A_{2g}$ photoreaction, since reaction and emission are competitive processes out of this excited level. However, for Rh(III) systems where the ^3E_g sublevel lies lower, *non*reactive radiationless processes are often the dominant ^3E_g relaxation pathways.[25] We have noted for *trans*-Rh(cyclam)$(CN)_2^+$ that since the lower lying $^3A_{2g}$ level involves excitation in the in-plane amine positions, the macrocyclic ring may minimize the distortion normally expected in the equilibrated triplet level. The absence of significant distortion may significantly reduce the rate constants for $^3A_{2g}$ radiationless deactivation processes.[26] A clearer assessment of the actual role played by the tet a and cyclam macrocyclic rings may be possible from a study of the photobehavior of *trans*-Rh(en)$_2$(CN)$_2^+$, which also has a lower lying $^3A_{2g}$ level.

Conclusion

The present findings are similar to those previously observed for related Cr(III) and Rh(III) complexes with the macrocyclic ligand cyclam.[1,4,5] It appears that steric and electronic factors associated with the additional presence in the tet a ligand of six methyl groups on the ring periphery have only a small influence on the photophysical and photochemical properties of these complexes.

Acknowledgment. We gratefully acknowledge the Research Corp. and the Camille and Henry Dreyfus Foundation for support of this work. This study was also supported by a National Science Foundation Grant (No. PRM-8109082).

Registry No. *trans*-[Cr(teta)(CN)$_2$]ClO_4, 101347-93-7; *trans*-[Cr(teta)$(NO_3)_2$]NO_3, 101374-85-0; *trans*-[Cr(teta)$(NH_3)_2$]$(PF_6)_3$, 101347-95-9; *trans*-[Rh(teta)Cl_2]ClO_4, 101469-38-9; *trans*-[Rh(teta)(CN)$_2$]ClO_4, 101375-05-7; *trans*-[Cr(teta)Cl_2]ClO_4, 86916-01-0.

(23) Endicott, J. F. *J. Chem. Educ.* **1983**, *60*, 824.
(24) Ditze, A.; Wasgestian, F. *J. Phys. Chem.* **1985**, *89*, 426.
(25) Bergkamp, M. A.; Brannon, J.; Madge, D.; Watts, R. J.; Ford, P. C. *J. Am. Chem. Soc.* **1979**, *101*, 4549; Bergkamp, M. A.; Watts, R. J.; Ford, P. C. *J. Phys. Chem.* **1981**, *85*, 684.
(26) We thank John DiBenedetto for bringing this latter point to our attention (private communication).
(27) Zinato, E.; Adamson, A. W.; Reed, J. L.; Puaux, J. P.; Riccieri, P. *Inorg. Chem.* **1984**, *23*, 1138.

Contribution from the Laboratoire de Chimie de Coordination, UA 416 CNRS, Université Louis Pasteur, F-67070 Strasbourg Cêdex, France, and Fakultät für Chemie, Universität Bielefeld, D-4800 Bielefeld 1, FRG

Crystal Structures of the Tetra-*n*-butylammonium Salts of the $AuCl_2^-$, $AuBr_2^-$, and AuI_2^- Ions

Pierre Braunstein,*[1a] Achim Müller,*[1b] and Hartmut Bögge[1b]

Received November 13, 1985

The dihaloaurate(I) complex ions $[AuX_2]^-$ (X = Cl, Br, I) have been known for some time[2,3] although their systematic synthesis and isolation as tetraalkylammonium salts were only achieved quite recently, according to reactions 1–3.[4]

$$2[R_4N][AuCl_4] + PhNHNH_2{\cdot}HCl \rightarrow [R_4N][AuCl_2] + [R_4N][PhAuCl_3] + N_2 + 4HCl \quad (1)$$

$$[R_4N][AuBr_4] + CH_3COCH_3 \rightarrow [R_4N][AuBr_2] + BrCH_2COCH_3 + HBr \quad (2)$$

$$[R_4N][AuBr_2] + 2[R_4N]I \rightarrow [R_4N][AuI_2] + 2[R_4N]Br \quad (3)$$

These reactions involve the easily available ionic precursors $AuCl_4^-$ and $AuBr_4^-$ and selective reducing agents. Thus, phenylhydrazine was used in reaction 1 because it is less reducing than hydrazine, which would lead to metallic or colloidal gold. The mechanism of this interesting reaction, which also led to the arylgold(III) complex $[PhAuCl_3]^-$, has been investigated and found to involve a 1,2-shift of the phenyl ring from a nitrogen atom of $PhNHNH_2$ to the gold center via a coordinated nitrene intermediate.[5] Reaction 2 is very clean since the organic product formed upon oxidation of acetone is volatile. This reaction is

(1) (a) Université Louis Pasteur. (b) Universität Bielefeld.
(2) Puddephatt, R. J. In *The Chemistry of Gold*; Clark, R. J. H., Ed.; Topics in Inorganic and General Chemistry; Elsevier: Amsterdam, 1978; Vol. 16.
(3) Schmidbaur, H. *Angew. Chem., Int. Ed. Engl.* **1976**, *15*, 728.
(4) Braunstein, P.; Clark, R. J. H. *J. Chem. Soc., Dalton Trans* **1973**, 1845.
(5) Braunstein, P. *J. Chem. Soc., Chem. Commun.* **1973**, 851.

0020-1669/86/1325-2104$01.50/0

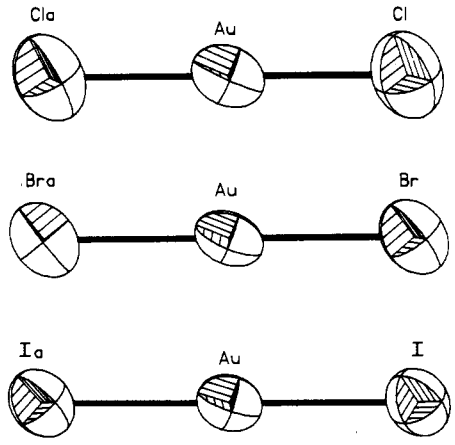

Figure 1. Structures of the $[AuX_2]^-$ anions in the $[n\text{-}Bu_4N][AuX_2]$ (X = Cl, Br, I) complexes.

quantitative, like reaction 3, which involves a conventional metathetical exchange between Br^- and I^-.[4]

These complexes were shown to be valuable precursors for the synthesis of metal–metal-bonded heterotrinuclear chain complexes of the type [M–Au–M]$^-$, where M represents a metal carbonyl fragment.[6,7] The availability of the $[R_4N][AuX_2]$ complexes has also allowed various spectroscopic techniques to be applied to them: e.g., infrared,[4] Raman,[4] ^{197}Au Mössbauer,[7,8] ^{35}Cl and ^{37}Cl nuclear quadrupole resonance,[9,10] X-ray photoelectron,[11] and electronic and magnetic circular dichroism.[12] The results were all consistent with a linear coordination about the gold center, as expected for a two-coordinated d^{10} sp-hydridized ion.

Here we present and compare the results of the crystal structure determinations of the $[n\text{-}Bu_4N][X\text{–}Au\text{–}X]$ complexes (X = Cl, Br, and I).

Results and Discussion

The results of the crystal structure determinations of the complexes $[n\text{-}Bu_4N][AuX_2]$ (X = Cl, (**1**), X = Br (**2**), X = I (**3**)) confirm the linearity of the gold(I) coordination since the metal occupies a center of inversion in these anions (Figure 1). The $[n\text{-}Bu_4N]^+$ cation lies on a twofold axis and presents no unusual features or contacts. The Au–Cl distance in **1** [225.7 (4) pm] is shorter than that found for the $[AuCl_2]^-$ anion in the mixed-valence complexes $Cs_2[AuCl_2][AuCl_4]$ [228.1 (2) pm][13] or $Rb_3[AuCl_2]_2[AuCl_4]$ [226, 227 (4) pm].[14] The Au–Br distance in **2** [237.6 (3) pm] is longer than that found for the $[AuBr_2]^-$ anion in the mixed-valence species $[Au(S_2CNBu_2)_2][AuBr_2]$ [234.9 (5) pm][15] and shorter than in $Rb_2[AuBr_2][AuBr_4]$ [240.2 (8) pm].[14] The Au–I distance in **3** [252.9 (1) pm] is shorter than that found for the $[AuI_2]^-$ anion in the mixed-valence species $K_2[AuI_2][AuI_4]$ [256.4 (3) pm][16] or $Rb_2Ag[AuI_2]_2[AuI_4]$ [257.0 (9) and 254.9 (9) pm].[17] Obviously, counterion effects, electronic perturbations, and packing forces can significantly affect Au–X values. It is therefore necessary to compare values within a homologous series of discrete entities.

The Au–X distances in **1–3** are all shorter than the sum of the corresponding atomic radii:[18] 232.6, 247.6, and 266.6 pm, respectively. The difference between each set of corresponding values increases of going from Cl to I (Δ = 6.9, 10.0, and 13.7 pm), paralleling the increase in covalent character along the series $AuCl_2^- < AuBr_2^- < AuI_2^-$.

This conclusion was also reached when the stretching force constants within the $[n\text{-}Bu_4N][AuX_2]$ series were compared.[4]

As expected from the bridging nature of the halides in polymeric $(AuX)_n$, the corresponding Au–X distances (Au–Cl = 236 pm,[19] Au–Br = 240, 244 pm,[20] Au–I = 262 pm[21]) are longer than in the discrete $[AuX_2]^-$ anions.

Table I. Summary of Crystal Data and Intensity Data Collection

compd	$[n\text{-}Bu_4N][AuCl_2]$	$[n\text{-}Bu_4N][AuBr_2]$	$[n\text{-}Bu_4N][AuI_2]$
empirical formula	$C_{16}H_{36}AuCl_2N$	$C_{16}H_{36}AuBr_2N$	$C_{16}H_{36}AuI_2N$
cryst dimens, mm	0.2 × 0.5 × 0.5	0.1 × 0.2 × 0.25	0.3 × 0.4 × 0.5
space group	$C2/c$	$C2/c$	$C2/c$
a, pm	1306.9 (3)	1303.1 (3)	1300.9 (4)
b, pm	998.3 (2)	1026.7 (3)	1066.5 (3)
c, pm	1597.3 (4)	1611.2 (4)	1641.2 (5)
β, deg	92.72 (2)	93.15 (2)	93.48 (3)
V, pm^3	2081.6 × 10^6	2152.2 × 10^6	2272.8 × 10^6
Z	4	4	4
d_{calcd}, g·cm^{-3}	1.63	1.85	2.03
μ(Mo Kα), cm^{-1}	73.08	104.97	91.46
F(000), electrons	1008	1152	1296
diffractometer	Syntex $P2_1$ four circle		
radiation	Mo Kα (λ = 71.069 pm; graphite monochromator)		
reflcns measd	$+h,+k,\pm l$	$+h,+k,\pm l$	$+h,+k,\pm l$
scan mode	ω scan	ω scan	ω scan
scan range, (2θ), deg	4–54	4–54	4–54
scan width	1° in ω bisected by K$\alpha_{1,2}$ maximum		
scan speed, deg·min^{-1}	3.5–29.3	2.9–29.3	3.5–29.3
bkgd/scan time ratio	0.6	0.66	0.6
temp, K	294	294	294
check reflcns	1 reflcn every 39 reflections		
no. of measd reflcns	2585	2671	2802
no. of unique obsd reflcns ($F_o > 3.92\sigma(F_o)$)	1725	1435	1893
weighting scheme	$1/\sigma^2(F_o)$	$1/\sigma^2(F_o)$	$1/\sigma^2(F_o)$
no. of variables	93	93	93

Table II. Atom Coordinates and Temperature Factors (10^4 pm^2) for $[n\text{-}Bu_4N][AuCl_2]$

atom	x	y	z	U^a
Au	0.2500	0.2500	0.0000	0.068 (1)
Cl	0.2723 (4)	0.4369 (5)	0.0783 (2)	0.101 (2)
N	0.5000	0.1486 (12)	0.2500	0.042 (4)
C1	0.4869 (8)	0.2402 (12)	0.3260 (6)	0.049 (3)
C2	0.4732 (10)	0.1710 (12)	0.4080 (6)	0.056 (4)
C3	0.4391 (10)	0.2764 (12)	0.4699 (6)	0.065 (5)
C4	0.4159 (11)	0.2063 (15)	0.5576 (7)	0.086 (6)
C5	0.4077 (7)	0.0572 (11)	0.2337 (6)	0.047 (3)
C6	0.3036 (8)	0.1271 (12)	0.2288 (7)	0.055 (4)
C7	0.2267 (8)	0.0372 (13)	0.1923 (7)	0.060 (4)
C8	0.1222 (10)	0.1030 (14)	0.1873 (9)	0.082 (6)

[a] Equivalent isotropic U defined as one-third of the trace of the orthogonalized U_{ij} tensor.

Experimental Section

Single crystals of **1–3** were obtained as described in the literature.[4]

(6) Braunstein, P.; Dehand, J. *J. Organomet. Chem.* **1975**, *88*, C24.
(7) Braunstein, P.; Schubert, U.; Burgard, M. *Inorg. Chem.* **1984**, *23*, 4057.
(8) Parish, R. V. *Gold Bull.* **1982**, *15*, 51.
(9) Bowmaker, G. A.; Whiting, R. *Aust. J. Chem.* **1976**, *29*, 1407.
(10) Jones, P. G.; Williams, A. F. *J. Chem. Soc., Dalton Trans* **1977**, 1430.
(11) McNeillie, A.; Brown, D. H.; Smith, W. E.; Gibson, M.; Watson, L. *J. Chem. Soc., Dalton Trans* **1980**, 767.
(12) Koutek, M. E.; Mason, W. R. *Inorg. Chem.* **1980**, *19*, 648.
(13) Eijndhoven, J. C. M. T.; Verschoor, G. C. *Mater. Res. Bull.* **1974**, *9*, 1667.
(14) Strähle, J.; Gelinek, J.; Kölmel, M. *Z. Anorg. Allg. Chem.* **1979**, *456*, 241.
(15) Beurskens, P. T.; Blaauw, H. J. A.; Cras, J. A.; Steggerda, J. J. *Inorg. Chem.* **1968**, *7*, 805.
(16) Strähle, J.; Gelinek, J.; Kölmel, M.; Nemecek, A. M. *Z. Naturforsch., B* **1979**, *34B*, 1047.
(17) Werner, W.; Strähle, J. *Z. Naturforsch., B* **1979**, *34B*, 952.
(18) Holleman-Wiberg, *Lehrbuch der Anorganischen Chemie*; Walter de Gruyter: Berlin, 1985.
(19) Janssen, E. M. W.; Folmer, J. C. W.; Wiegers, G. A. *J. Less-Common Met.* **1974**, *38*, 71.
(20) Janssen, E. M. W.; Wiegers, G. A. *J. Less-Common Met.* **1978**, *57*, 47.
(21) Weiss, A.; Weiss, A. *Z. Naturforsch., B* **1956**, *11B*, 604. Jagodzinski, H. *Z. Krist.* **1959**, *112*, 80.

Table III. Atom Coordinates and Temperature Factors (10^4 pm^2) for [*n*-Bu_4N][$AuBr_2$]

atom	*x*	*y*	*z*	U^a
Au	0.2500	0.2500	0.0000	0.062 (1)
Br	0.2790 (2)	0.4462 (3)	0.0758 (2)	0.088 (1)
N	0.5000	0.1447 (23)	0.2500	0.043 (8)
C1	0.4849 (13)	0.2332 (20)	0.3232 (11)	0.047 (6)
C2	0.4724 (14)	0.1703 (19)	0.4058 (11)	0.050 (7)
C3	0.4358 (15)	0.2638 (23)	0.4689 (12)	0.061 (8)
C4	0.4246 (17)	0.1994 (26)	0.5556 (15)	0.098 (12)
C5	0.4078 (11)	0.0588 (19)	0.2349 (11)	0.044 (7)
C6	0.3047 (13)	0.1255 (21)	0.2241 (13)	0.055 (8)
C7	0.2212 (13)	0.0317 (24)	0.1928 (13)	0.064 (9)
C8	0.1158 (14)	0.0917 (23)	0.1866 (17)	0.088 (11)

[a] Equivalent isotropic *U* defined as one-third of the trace of the orthogonalized U_{ij} tensor.

Table IV. Atom Coordinates and Temperature Factors (10^4 pm^2) for [*n*-Bu_4N][AuI_2]

atom	*x*	*y*	*z*	U^a
Au	0.2500	0.2500	0.0000	0.064 (1)
I	0.2888 (1)	0.4539 (1)	0.0743 (1)	0.082 (1)
N	0.5000	0.1397 (11)	0.2500	0.049 (4)
C1	0.4842 (7)	0.2236 (9)	0.3221 (6)	0.054 (3)
C2	0.4757 (8)	0.1605 (11)	0.4030 (6)	0.060 (4)
C3	0.4340 (9)	0.2485 (11)	0.4649 (7)	0.069 (4)
C4	0.4273 (11)	0.1954 (11)	0.5505 (7)	0.082 (5)
C5	0.4069 (6)	0.0537 (10)	0.2326 (6)	0.056 (3)
C6	0.3037 (7)	0.1160 (11)	0.2199 (6)	0.059 (4)
C7	0.2221 (8)	0.0287 (11)	0.1872 (7)	0.074 (4)
C8	0.1180 (8)	0.0848 (14)	0.1821 (8)	0.096 (6)

[a] Equivalent isotropic *U* defined as one-third of the trace of the orthogonalized U_{ij} tensor.

The structures of [*n*-Bu_4N][$AuCl_2$] (**1**), [*n*-Bu_4N][$AuBr_2$] (**2**), and [*n*-Bu_4N][AuI_2] (**3**) were determined from single-crystal data (Syntex $P2_1$ four-circle diffractometer). Summaries of the crystal data and details concerning the intensity data collection are given in Table I. The unit cell parameters were obtained at 21 °C by a least-squares refinement of the angular settings of 15 high-angle reflections. An empirical absorption correction was applied for **1** and **3**. As the crystal of **2** moved in the glass tube, in which it had been sealed, just after the intensity data were collected, no absorption correction could be applied for **2**. The data were corrected for Lorentz and polarization effects.

The structures were solved by conventional heavy-atom methods (the SHELXTL program package was used for **1**, **2**, and **3**). After detection of the heavy atoms the positional parameters of the remaining non-hydrogen atoms were deduced from successive difference Fourier syntheses. The CH_2 and CH_3 units of the *n*-Bu_4N^+ cation were refined as rigid groups with hydrogen atoms riding on the carbon atoms (C–H = 96 pm).

The final least-squares refinement converged respectively at $R = \sum||F_o| - |F_c||/\sum|F_o| = 0.052$ (**1**), 0.090 (**2**), and 0.047 (**3**) and $R_w = (\sum w(|F_o| - |F_c|)^2/\sum w|F_o|^2)^{1/2} = 0.056$ (**1**), 0.074 (**2**), and 0.045 (**3**), where $1/w = \sigma^2(F_o)$. During the last cycles of refinement no parameter shifted more than 0.1σ, where σ is the standard deviation of the parameter.

The atomic scattering factors for all atoms were taken from standard sources.[22] Anomalous dispersion corrections were applied to all atoms. Positional and thermal parameters for **1**, **2**, and **3** are given in Tables II–IV. Tables of anisotropic thermal parameters, calculated hydrogen atom positions, complete bond lengths and angles, and lists of observed and calculated structure factors are available as supplementary material.

Acknowledgment. P.B. is grateful to the CNRS and Université Louis Pasteur for financial support and to Johnson-Matthey and Co. Ltd. for a generous loan of $Na[AuCl_4]\cdot xH_2O$.

Note Added in Proof. Further Au–I distances have recently been determined: 256.5 (2) pm[23] in $[Au\{\overline{S(CH_2)_3CH_2}\}I]_\infty$ and 256.10 (6) pm[24] in the superconductor β-$(ET)_2AuI_2$ ("ET" is bis(ethylenedithio)tetrathiafulvalene).

Registry No. **1**, 50480-99-4; **2**, 50481-01-1; **3**, 50481-03-3.

Supplementary Material Available: Complete bond lengths (Table S.I) and bond angles (Table S.II), anisotropic temperature factors (Table S.III), and hydrogen coordinates (Table S.IV) (5 pages). Ordering information is given on any current masthead page. According to policy instituted Jan 1, 1986, the tables of calculated and observed structure factors are being retained in the editorial office for a period of 1 year following the appearance of this work in print. Inquiries for copies of these materials should be directed to the Editor.

(22) *International Tables for X-Ray Crystallography*; Kynoch: Birmingham, England, 1974; Vol. IV.
(23) Ahrland, S.; Norén, B.; Oskarsson, Å. *Inorg. Chem.* **1985**, *24*, 1330.
(24) Wang, H. H.; Beno, M. A.; Geiser, U.; Firestone, M. A.; Webb, K. S.; Nuñez, L.; Crabtree, G. W.; Carlson, K. D.; Williams, J. M.; Azevedo, L. J.; Kwak, J. F.; Schirber, J. E. *Inorg. Chem.* **1985**, *24*, 2465.